Schwintzer, P., Kang, Z., Reigber, C., Zhu, S. Y. (1994): Deterministic Simulation of Global Gravity Field Recovery from STEP - GPS SST Data, and Oceanographic Implacations, 105-118. - In: Rummmel and Schwintzer (Eds.): A Major STEP for Geodesy. Report 1994 of the STEP Geodey Working Group, Munich, Potsdam, Germany, November, 1994

DETERMINISTIC SIMULATION OF GLOBAL GRAVITY FIELD RECOVERY FROM STEP - GPS SST DATA, AND OCEANOGRAPHIC IMPLICATIONS

P. Schwintzer, Z. Kang, Ch. Reigber, S.Y. Zhu
GeoForschungsZentrum (GFZ) Potsdam, Dept. 1, Germany

ABSTRACT

The new tracking scenario, i.e. satellite-to-satellite tracking (SST) between the high-altitude GPS satellites and a low-flying spacecraft, was realized for geodetic applications with the American/French altimeter mission TOPEX/Poseidon. Because of its capability to provide continous data coverage, GPS space-based tracking for precise orbit determination is superior to any ground-based system. TOPEX/Poseidon-GPS SST data was recently evaluated at GFZ for use in global gravity field model improvement. It turned out that due to the relative large altitude (1336 km) of TOPEX/Poseidon the contribution to existing state-of-the-art gravity field models is perceivable but not very singificant. The same tracking and computation scenario was simulated for a very low-flying drag-free satellite, like STEP, with an orbit altitude of 450 km. The actual result proves that from STEP-GPS SST data, taken only over a 9-day period, a complete and almost perfect recovery of all spectral terms up to degree/order 25 of the global gravity field is possible, assuming no errors but data noise. It must be pointed out that this solution is got from only one satellite whereas existing satellite-only gravity field models are derived form orbit perturbation analyses of some 30 satellites flying in different orbits. The accumulative geoid error for a spectral resolution of degree/order 25 is 3 cm for the STEP simulation solution and 70 cm for state-of-the-art global gravity field models, respectively. This implies that with a STEP-like mission the geoid-induced velocity errors in altimetry-derived geostrophic ocean currents can be reduced to a level of a few mm/s and well below 1 mm/s for the very long-wavelength parts up to degree/order 10. Repeating the computations but applying a realistic error model, taking into account e.g. residual air drag and GPS ephemerides errors, degrade the accuracy by about a factor of 5 (geoid) to 10 (ocean currents).

INTRODUCTION

Numerous simulation studies performed for the ARISTOTELES and STEP mission concepts [e.g. Rummel, Schrama 1991; Schrama 1992; Visser et al. 1994] have demonstrated the potential of GPS satellite-to-satellite tracking in gravity field recovery, if employed on a very low-flying satellite. The objective of this study is to verify in a first attempt the results, obtained so far from covariance analyses, applying now a purely deterministic approach: classical dynamic orbit computation and orbit perturbation evaluation based upon simulated GPS satellite-to-satellite tracking data. At present, the limitations of the deterministic approach are due to the computational burden, caused by the huge amount of data points to be processed for a full 6-month mission simulation, and due to the large number of gravitational unknowns to be solved for a medium resolution global gravity field model. For these reasons the following investigations are restricted to the long-wavelength part of the Earth gravity field ($\lambda/2 \approx 700$ km, spatial resolution at the Earth surface) and a short observation period of 9 days. The principle questions addressed are:

- Does a STEP-like mission allow to recover the global gravity field from one satellite only?

- Is the gain in geoid accuracy and resolution w.r.t. present-day global gravity field models significant to make a major contribution in resolving geostrophic ocean current flow from altimeter data?

STEP PRECISE ORBIT DETERMINATION AND GRAVITY FIELD RECOVERY - SOLUTION STRATEGY

The approach chosen at GFZ to evaluate the GPS data collected from the ground station receivers and the satellite on-board receiver over a given time period is characterized by using undifferenced pseudorange and carrier phase measurements and a processing split up into two sequential parts: GPS orbit and clock parameter estimation from the GPS ground station network data followed by the evaluation of the satellite-to-satellite tracking data. Due to GFZ's engagement in the International GPS Geodynamics Service (IGS) [Beutler et al 1994], the ephemerides and clock parameters of the full constellation of some 20 GPS satellites are routinely estimated from the observations collected from the global IGS-network [Gendt et al 1994]. One observation period was selected to provide the predetermined 'real' GPS ephemerides and clock parameters for use in the simulations described below.

The GPS satellites' ephemerides and clock parameters, which have an approximate accuracy of 20 cm and 1ns, respectively, are introduced as fixed parameters in the low-altitude satellite orbit computation. The in-house developed software EPOS numerically integrates the satellite equations of motion from a nominal initial state within a given force field and reference frame, computes partial derivatives of the observations w.r.t. the selected solve-for parameters, either explicitely or by integrating the variational equations, and solves for the unknown parameters in a least squares adjustment. Due to neglecting higher order terms in the linear formulation of the observation equations and because of the automatic editing the final solution is found after several iterations.

After convergence of an individual arc adjustment, the normal equation system is generated in a subsequent step with the gravitational parameters as additional unknowns. The normal equation system then is reduced for the arc-dependent parameters i.e. state vector, receiver clock biases and ambiguities. Eventually the reduced normal equation systems are accumulated over the whole observation period to yield the final gravity field model normal equation system which is solved by matrix inversion.

For the generation of the STEP normal equation system, normals from six 1.5-day orbit arcs are generated, covering the 9-day observation period. The adoption of an arclength of 1.5 days rather than 2- or 3-days has proven to give the best results.

The observables used are pseudoranges φ and carrier phases Φ fullfilling the following functional model [Hofmann-Wellenhof 1992]:

$$\varphi = /\underline{R} - \underline{r}/ + c \cdot dT - c \cdot dt + \varepsilon(\varphi) \tag{1}$$

$$\Phi = /\underline{R} - \underline{r}/ + c \cdot dT - c \cdot dt + \lambda \cdot N + \varepsilon(\Phi) \tag{2}$$

with

$\varphi = \varphi(t)$, $\Phi = \Phi(t)$	:	dual-frequency ionosphere-free combinations of pseudorange and phase, resp.
$R = R(t)$	:	GPS satellite position vector
$r = r(t)$	:	STEP satellite position vector
c	:	velocity of light
$dT = dT(t)$	:	GPS satellite clock bias
$dt = dt(t)$	:	STEP GPS receiver clock bias
λ	:	carrier signal wavelength
$N = N(t)$	:	ambiguity (number of full carrier cycles)
$\varepsilon = \varepsilon(t)$	:	measurement error

Both GPS observables can be characterized as biased range measurements. As the noise of the pseudoranges is by one to several orders larger than those of the phase measurements [Bertiger et al 1993], for precise applications the phase is the primary observable whereas the P-ranging code derived pseudoranges strengthen the solution through supporting the ambiguity resolution.

BASELINE ASSUMPTIONS FOR 'REAL-WORLD' SIMULATION OF STEP ORBIT AND GPS-SST OBSERVATIONS

The adopted study-relevant force field and geometric models, the orbit and satellite parameters underlying the integration of the 'true' STEP-like orbit are summarized in Table 1. Figure 1 shows the resulting ground-track pattern over the 9-day data evaluation period. Using the generated 'true' orbit and the IGS (GFZ)-ephemerides of the GPS satellites, the observables phase and pseudoranges are generated applying only random noise. The on-board GPS receiver assumptions and the resulting observation statistics are given in Table 2.

Table 1. STEP orbit simulation - underlying models and orbit configuration.

Parameter	Model/Value
Dynamic Model	
Static gravitational geopotential	GRIM4-C3 [Schwintzer et al. 1993] truncated after degree/order 30
Ocean tides	GRIM4-C3 combined with Schwiderski (19,4) spherical harmonic model (12 tides)
Atmospheric drag	drag-free
Geometric Model	
GPS satellite ephemerides, GPS satellite clock biases	IGS (GFZ)
STEP Orbit and Satellite	
Sun-synchronous	
Repeat-cycle	~ 2 months (3-day subcycle)
Semi-major axis	6826 km
Mean altitude	448 km
Inclination	97.565°
Eccentricity	.001
RA of ascending node	shift after each 3 days to get regular ground-track pattern over a 9-day period
Satellite body	cube (4 m^2)
Satellite mass	800 kg

Table 2. STEP orbit simulation - observation model and statistics.

Parameter	Processing
Receiver channels	12
Antenna field of view	full sphere
Epochs	1993, Feb. 8, 9.5, 11, 12.5, 14, 15.5
Observation rate	60 s
Arc length	36 hours
Data noise	phase: 5 mm, pseudorange: 5 cm
data points per arc	$\sim$ 2·24000 phase and pseudorange

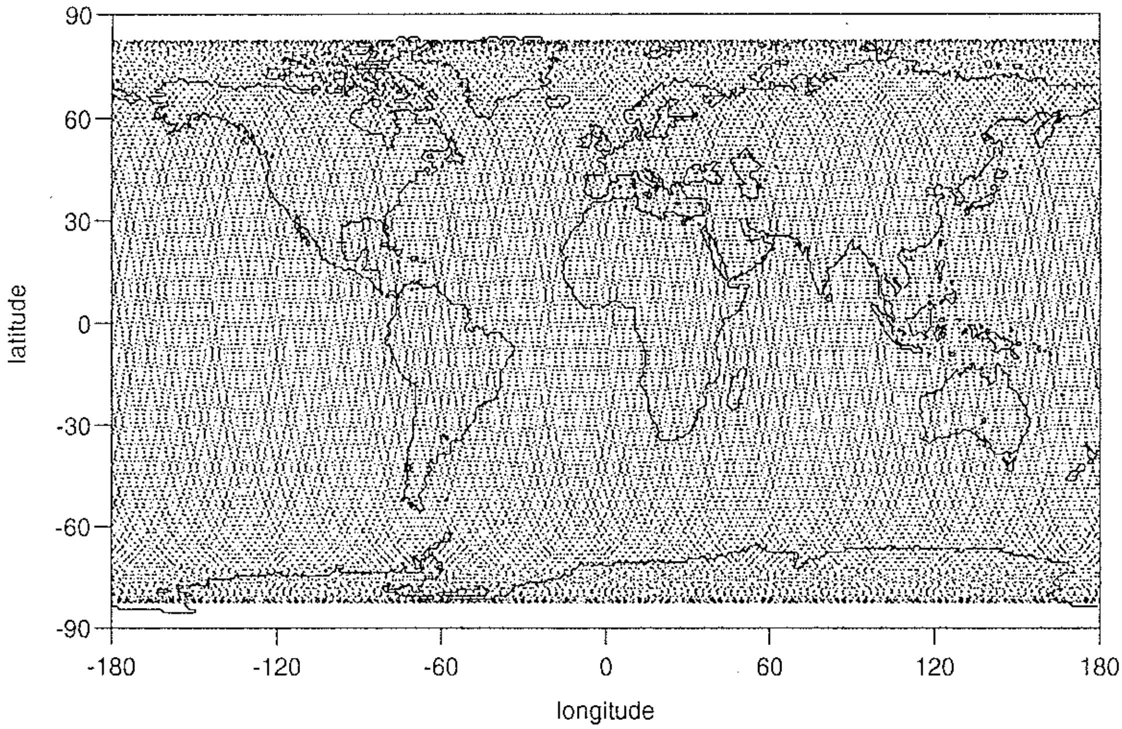

Figure 1. STEP ground tracks (9 days)

GRAVITY FIELD RECOVERY FROM STEP-GPS SST DATA

Two tests have been performed to recover the GRIM4-C3 satellite/surface data combined gravity field model from the simulated STEP-GPS satellite-to-satellite data. The first test doesn't take into account apart from measurement noise any other disturbing force or systematic error but gravity: STEP orbit computation with the GRIM4-C3 gravity field model replaced by the American JGM2-S satellite-only gravity field model [Nerem et al. 1993], again truncated after degree/order 31.

The second test additionally takes into account simulated systematic errors induced by the ocean tidal potential, the fixed GPS ephemerides, and residual short-period air drag fluctuations. For these error simulations, the orbit computation for the gravity field normal equation systems are performed using the Schwiderski ocean tide model instead of the GRIM4-C3 model, and the GPS ephemerides, computed and distributed by JPL, instead of the GFZ ones. The air-drag fluctuations, which are beyond the frequency-bandwidth of the anticipated STEP drag-free system [Reinhard et al 1993], are assumed, following a study of Touboul et al. (1991), to reach 10 % of the DTM [Barlier et al. 1978] air density over a 2-min period. This impuls is introduced during STEP's orbit restitution 4-times per revolution at /75°/-latitude with changing sign after each revolution.

The orbit errors induced by the systematic errors in the 2nd test amount to about 20 cm, whereas in the first case a purely gravitational orbit can be exploited for gravity field recovery (c.f. Table 3). The gravitational signal in the STEP orbit (difference JGM2-S to GRIM4-C3) is of the order of 4 m. Table 4 lists the solve-for parameters considered in the orbit computations and the generation of normal equation systems.

Table 3. Effect of measurement noise and model errors in STEP's orbit computation ('real' vs. 'recovered').

error source	**position (rms)** [cm]			**orbital fit (rms)** [cm]	
	radial	along-track	across-track	phase	pseudorange
Test 1:					
measurement noise	0.0	0.1	0.0	0.4	5.0
Test 2:					
GPS ephemerides (GFZ vs. JPL)	1.7	3.7	1.8	5.6	17.7
ocean tides (GRIM4 vs. Schwiderski)	0.9	1.9	2.9	1.4	3.0
air density fluctuations	4.6	15.8	0.5	4.6	28.1
geopotential (GRIM4-C3 vs JGM2-S)	170	370	120	90	420

Table 4. Solve-for parameters in STEP orbit and gravity field recovery.

Parameter	Parametrization
STEP state	position and velocity at initial epoch
Phase ambiguity	once per GPS satellite pass (~ 450 unknowns per arc)
On-board receiver clock bias	at each 1-min observation epoch (~ 2000 unknowns per arc)
JGM-2S (30/30) gravity field model	spherical harmonic coefficients up to degree/order 30

Results of Test 1 on Global Gravity Field Recovery (Noise-only Case)

It turned out, that due to the observations sampling rate and the ground track pattern, a resolution up to degree/order 30 could not be achieved. In order to overcome the undersampling effects, the gravitational coefficients with a degree higher than 25 were reduced before accumulation in each of the six 1.5-day normal equation systems. The accumulation of the reduced systems, containing the remaining 674 gravitational coefficients up to degree/order 25, results in a stable normal equation system, which can be solved without adding any constraints for matrix stabilization. The a-posteriori standard deviation of unit weight exactly meets the a-priori value of 1.0.

The GRIM4-C3 (25/25) gravity field could be recovered to a mean difference of 3 cm in terms of geoid heights and 0.09 mgal in terms of gravity, compared to the initial difference (JGM2-S vs. GRIM4-C3) up to degree/order 25 of 70 cm and 1.9 mgal, respectively. The almost perfect recovery corresponds to estimates for geoid, gravity, and geoid induced ocean current velocity errors, derived by rigorous error propagation, which are about 1.5 orders of magnitude smaller than those for state-of-the-art satellite-only global gravity field models (represented by the latest GRIM4 model [Schwintzer et al. 1994]). All results are tabulated in Table 5 for both cases, accumulative errors up to degree/order 10 - the very long-wavelength part -, and up to maximum degree/order 25. One has to take into account that present-day global gravity field models are based upon several years of tracking of some 30 satellites compared to a 9-day tracking period with one satellite for the STEP solution.

To propagate the gravity field error to ocean current velocities, one starts with the formulas for the velocity field of ocean circulation in geostrophic approximation [Pedlosky 1987]:

$$\dot{x}(\varphi,\lambda) = -\frac{g}{f \cdot R} \cdot \frac{\partial h(\varphi,\lambda)}{\partial \varphi} \qquad (3)$$

$$\dot{y}(\varphi,\lambda) = \frac{g}{f \cdot R \cdot \cos\varphi} \cdot \frac{\partial h(\varphi \cdot \lambda)}{\partial \lambda} \tag{4}$$

with $\dot{x}\ (\varphi,\lambda)$ - west-east component of ocean current velocity
$\dot{y}\ (\varphi,\lambda)$ - south-north component of ocean current velocity
$\partial h\ (\varphi,\lambda)/\partial\varphi$ - gradient of sea surface topographic w.r.t. latitude
$\partial h\ (\varphi,\lambda)/\partial\lambda$ - gradient of sea surface topographic w.r.t. longitude
g - mean gravitational acceleration at the Earth's surface
f - horizontal component of Coriolis-force ($f = 2\ \Omega \sin\varphi$)
Ω - angular velocity of Earth's rotation
R - Earth's equatorial radius

If the sea surface topography is derived by satellite altimetry on the basis of an underlying geoid model, the geoid-induced standard deviation in the velocity components $\dot{x}$ and $\dot{y}$ is proportional to the standard deviations in the deflections of the vertical ($\xi = \xi\ (\varphi,\lambda)$ - south-north component, $\eta = \eta\ (\varphi,\lambda)$ - west-east component):

$$s_{\dot{x}} = \frac{g}{f} \cdot s_{\xi} \tag{5}$$

$$s_{\dot{y}} = \frac{g}{f} \cdot s_{\eta} \tag{6}$$

The deflections of the vertical are functions of the spherical harmonic coefficients $C_{l,m}$, $S_{l,m}$ of the gravitational geopotential [Wenzel 1985], whose variance-covariance-matrix is part of the adjustment result. Using the full variance-covariance-matrix, the coefficients errors are propagated according to the following law (in matrix notation):

$$s_{\xi}^2 = f^T\, V_{c,s}\, f \qquad \xi = f^T \begin{Bmatrix} C_{l,m} \\ S_{l,m} \end{Bmatrix} \tag{7}$$

$$s_{\eta}^2 = g^T\, V_{c,s}\, g, \qquad \eta = g^T \begin{Bmatrix} C_{l,m} \\ S_{l,m} \end{Bmatrix} \tag{8}$$

with $s_{\xi} = s_{\xi}(\varphi,\lambda)$, $s_{\eta} = s_{\eta}(\varphi,\lambda)$, $f = f\ (\varphi,\lambda)$, and $g = g\ (\varphi,\lambda)$

The standard deviations (7) and (8) are computed for mean values over a regular 5°x5° equal angular grid and eventually introduced into Equations (5) and (6).

The requirement postulated by Martel, Wunsch (1993) for a ocean current velocity resolution of better than 10 mm/s, applying geodetic methods, is well achieved for the wavelengths covered by the simulated STEP solution (~ 0.2 mm/s up to degree/order 10, ~ 3 mm/s up to degree/order 25).

Figure 2 depicts the error degree variances of the STEP-SIM1 solution and a present-day satellite-only gravity field model vs. the geoid's signal degree variances. The geoid accuracy per degree stays below the 10 cm-threshold for the STEP-SIM1 solution whereas it is surpassed for existing solutions at about degree 10.

Results of Test 2 on Global Field Recovery (Noise plus Model Error Case)

The same computations as performed for Test 1 have been repeated, but this time introducing the systematic model errors as described above. The resulting normal equation system yields again a stable solution.

Due to the larger residuals, the a-posteriori standard deviation of unit weight now exceeds the a-priori value by a factor of 7.5. The accuracy of the gravity field solution is about a factor of 5 worse than in the error-free case. Nevertheless, from the only 9-day observation period the gravity field can be resolved up to degree/order 25 about 4 times as accurate as present-day satellite-only gravity field models: 16 cm vs. 70 cm, 0.5 mgal vs. 2 mgal, respectively. The geoid induced error in ocean current flow is on the mm/s-level for all terms up to degree/order 10 and increases to some cm/s for the degree/order 25 field, still a gain in accuracy w.r.t. present-day gravity field model of about a factor 10 to 2, depending on the resolution.

The solution is evaluated, applying the same error computations as for Test 1, with the numerical results tabulated in Table 6.

Figure 3 depicts the error degree variances of the STEP-SIM2 solution and a present-day satellite-only gravity field model vs. the geoid's signal degree variances. The 10 cm-threshold in the geoid accuracy per degree is surpassed with degree 25 for the STEP-SIM2 solution compared to about degree 10 for existing solutions.

CONCLUSIONS

Apart from all other perturbing forces and observation errors but gravity and noise, a stable and almost perfect gravity field recovery is possible complete up to degree/order 25 from only 9 days GPS-STEP (450 km) - SST data with about 1.5 orders of magnitude improvement in accuracy as compared to present-day global gravity field models (which are based upon several years of tracking of some 30 satellites).

Taking into account realistic systematic errors (GPS ephemerides, ocean tides, air-drag fluctuation) leads to a degradation in the accuracy of the gravity field model by a factor of about 5 w.r.t. to the error-free case.

The geoid-induced velocity errors in altimetry-derived geostrophic ocean currents could be reduced to a few mm/s in the error-free case and to about a few cm/s for the error-affected case, allowing a resolution of quasi-stationary sea surface topography and geostrophic ocean currents, also in the latter case, which is more than twice as much higher than with present-day global geiod models (degree/order 25 vs. degree/order 10).

The right choise of the arclength is a crucial point in gravity field recovery. Trying full solutions with normal equations generated from 6 x 1.5-day arcs, 5 x 2-day arcs and 3 x 3-day arcs, respectively, yielded best results for the 1.5-day case, slightly degraded results for the 2-day case, and unstable, meaningless results for the 3-d case.

Table 5: Results of test 1: rss of differences of recovered (STEP-SIM1) and initial (JGM2-S) gravity model to 'real-world' model, and accuracy of recovered solution vs. state-of-the-art satellite-only gravity model (GRIM4-S4).

	STEP-SIM1 (up to l,m = 10)	**JGM2-S** (up to l,m = 10)	**STEP-SIM1** (up to l,m = 25)	**JGM2-S** (up to l,m = 25)
Difference (rss) to 'real-world' model GRIM4-C3:				
geoid [cm]	0.3	10	3.0	70
gravity [μgal]	3	120	90	1900
	STEP-SIM1 (up to l,m = 10)	**GRIM4-S4*** (up to l,m = 10)	**STEP-SIM1** (up to l,m = 25)	**GRIM4-S4*** (up to l,m = 25)
Rigorous error propagation:				
geoid [cm]	0.2	11 ... 22	1.8 ... 2.9	26 ... 123
gravity [μgal]	2.5 ... 3	113 ... 225	65 ... 93	909 ... 3026
ocean current velocity				
west-east comp. [mm/s] $/\varphi/ = 85° \ldots 15°$	0.16 ... 0.74	7.7 ... 65	2.0 ... 13	36 ... 723
south-north comp. [mm/s] $/\varphi/ = 85° \ldots 15°$	0.15 ... 0.30	7.7 ... 18	1.8 ... 5.0	48 ... 231

* emprical scaling factor 5.5 applied

Table 6: Results of test 2: rss of differences of recovered (STEP-SIM2) and initial (JGM2-S) gravity model to 'real-world' model, and accuracy of recovered solution vs. state-of-the-art satellite-only gravity model (GRIM4-S4).

	STEP-SIM2 (up to l,m = 10)	**JGM2-S** (up to l,m = 10)	**STEP-SIM2** (up to l,m = 25)	**JGM2-S** (up to l,m = 25)
Difference (rss) to 'real-world' model GRIM4-C3:				
geoid [cm]	2.8	10	16	70
gravity [μgal]	30	120	500	1900
	STEP-SIM2 (up to l,m = 10)	**GRIM4-S4*** (up to l,m = 10)	**STEP-SIM2** (up to l,m = 25)	**GRIM4-S4*** (up to l,m = 25)
Rigorous error propagation:				
geoid [cm]	1.5 ... 1.7	11 ... 22	14 ... 22	26 ... 123
gravity [μgal]	18 ... 22	113 ... 225	490 ... 690	909 ... 3026
ocean current velocity				
west-east comp. [mm/s] $/\varphi/ = 85° ... 15°$	1.2 ... 5.5	7.7 ... 65	26 ... 180	36 ... 723
south-north comp. [mm/s] $/\varphi/ = 85° ... 15°$	1.0 ... 2.3	7.7 ... 18	23 ... 69	48 ... 231

* emprical scaling factor 5.5 applied

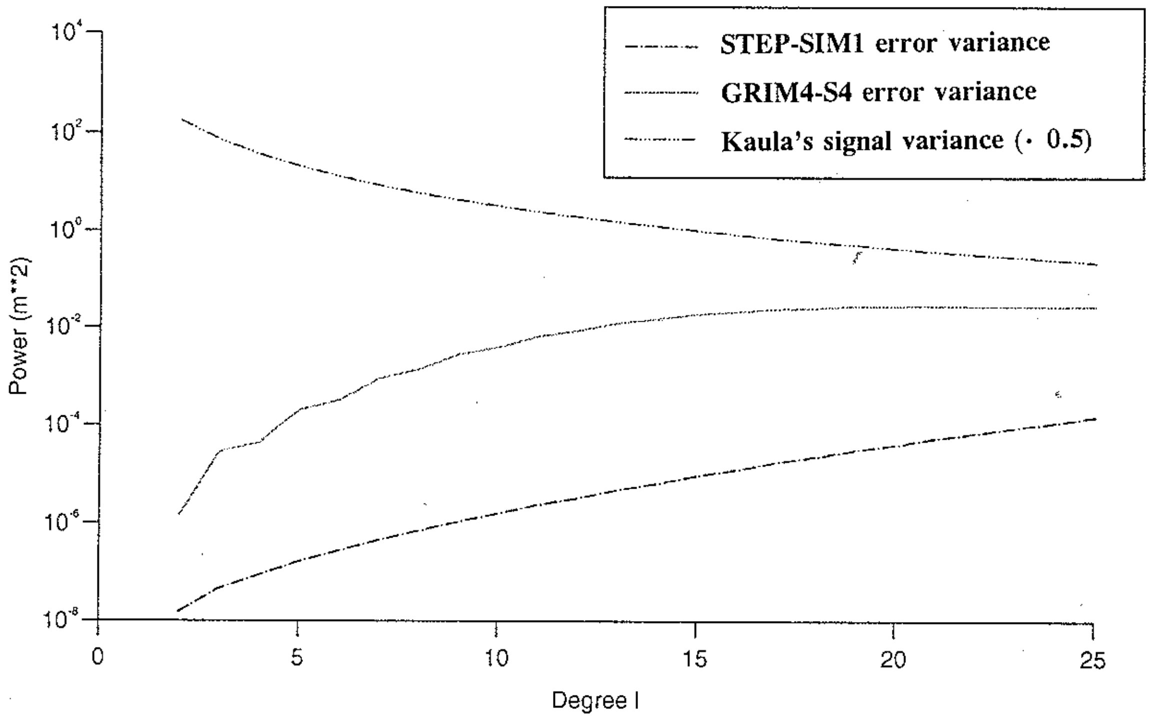

Figure 2. Error/Signal degree variances in terms of geoid heights (noise-only case).

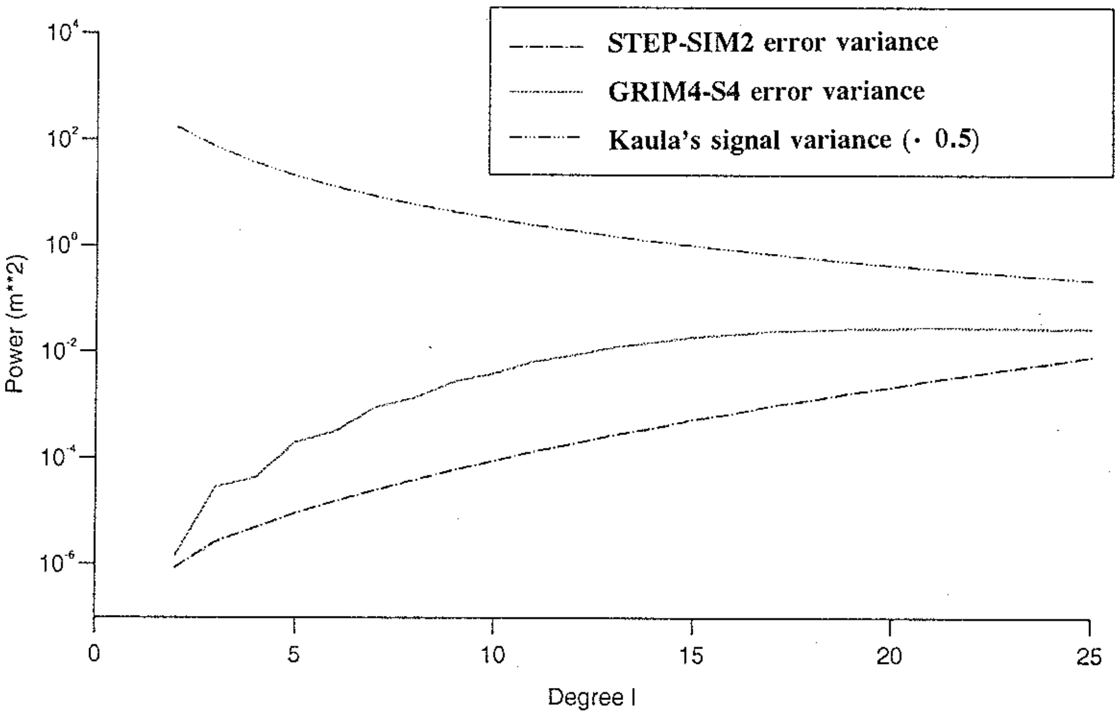

Figure 3. Error/Signal degree variances in terms of geoid heights (noise plus model error case).

Acknowledgement. This report is based on intermediate results obtained from GFZ's participation in the ongoing European Space Agency's 'Study of the Complementary Use of Gradiometry and Global Positioning System (GPS) for the Determination of the Earth's Gravity Field'. The study is supported by ESA under Grant RFQ/3-8017/93/F/Fl.

REFERENCES

Barlier, F., Berger, C., Falin, J., Kockarts, G., and G. Thuillier (1978). A Thermospheric Model Based Upon Satellite Drag Data, 9-24, *Ann. Geophys. 34.*

Beutler, G., Mueller, I.I., and R.E. Neilan (1994). The International GPS Service for Geodynamics (IGS): Development and Start of Official Service on 1 January 1994, 43-51, *Bulletin Géodésique 68.*

Bertiger, W.I., Bar-Sever, Y.E., Christensen, E.J., Davis, E.S., Guinn, J.R., Haines, B.J., Ibanez-Meier, R.W., Jee, J.R., Lichten, S.M., Melbourne, W.G., Muellerschoen, R.J. Munson, T.N., Vigue, Y., Wu, S.C., Yunck, T.P., Schutz, B.E., Abusali, P.A.M., Rim, H.J., Watkins, M.M. and P. Willis (1993). GPS Precise Tracking of TOPEX/Poseidon: Results and Implication, *J. Geophys. Res.,* special issue on TOPEX/Poseidon, submitted.

Gendt, G., Dick, G., Mai, W., Reigber, Ch., and Th. Nischan (1994). Earth Rotation Parameters and Station Coordinates from GPS Data, 3 pp, *IERS Annual Report 1994.*

Hofmann-Wellenhof, B., Lichtenegger, H., and J. Collins (1992). *Global Positioning System, Theory and Practice,* Springer.

Martel, F., and C. Wunsch (1993). Combined Inversion of Hydrography, Current Meter Data and Altimetric Elevations for the North Atlantic Circulation, 219-226, *manuscripta geodaetica* 18.

Nerem, R.S., Lerch, F.J., Marshall, J.A., Pavlis, E.C., Putney, B.H., Tapley, B.D., Eanes, R.J., Ries, J.C., Schutz, B.E., Shum, C.K., Watkins, M.M., Chan, J.C., Klosko, S.M., Luthcke, S.B., Patel, G.B., Pavlis, N.K., Williamson, R.G., Rapp, R.H., Biancale, R., and F. Nouel (1993). Gravity Model Development for TOPEX/Poseidon: Joint Gravity Models 1 and 2, *J. Geophys. Res.,* special issue on TOPEX/Poseidon, submitted.

Pedlosky, J. (1987). *Geophysical Fluid Dynamics*, Springer.

Reinhard, R., Jafry, V., and R. Laurance (1993). STEP-A Satellite Test of the Equivalence Principle, 251-263, *ESA Journal 17.*

Rummel, R., and E.J.O. Schram (1991). Two Complementary Systems On-board 'Aristoteles': Gradio and GPS, 135-139, *ESA Journal 15.*

Schrama, E.J.O. (1992). STEP Geodesy Co-experiment: New Results for an Orbit at 450 km Height, *Internal Memorandum*, Faculty of Geodetic Engineering, Delft.

Schwintzer, P., Reigber, Ch., Bode, A., Chen, Z., Massmann, F.H., Raimondo, J.C., Lemoine, J.M., Balmino, G., Biancale, R., Moynot, B., Marty, J.C., Barlier, F., and Y. Boudon (1993). Improvement of GRIM4 Earth Gravity Models Using GEOSAT Altimeter and SPOT-2 and ERS-1 Tracking Data, in Montag, H., and Ch. Reigber (eds.), *Geodesy and Physics of the Earth*, IAG Symp. No 112, Potsdam, Germany, Oct. 5-10, 1992, 11-20, Springer.

Schwintzer, P., Reigber, Ch., Bode, A., Kang, Z., Zhu, S.Y., Massmann, F.-H., Raimondo, J.C., Biancale, R., Balmino, G., Lemoine, J.M., Moynot, B., Marty, J.C., Barlier, F., and Y. Boudon (1994). Improvement of Global Gravity Field Modelling for ERS-1, Proceedings 2nd ERS-1 Symp. 'Space at the Service of our Environment', Hamburg 1993, *ESA SP-361*, 771-775, Noordwijk, The Netherlands.

Touboul, P., Bernard, A., Barlier, F., and C. Berger (1991). Air Drag Effect on Gradiometer Measurement, 73-91, *manuscripta geodaetica 16.*

Wenzel, H.-G. (1985). *Hochauflösende Kugelfunktionsmodelle für das Gravitationspotential der Erde*, Wissenschaftliche Arbeiten der Fachrichtung Vermessungswesen der Univ. Hannover, Nr. 137.